An Accurate On-Wafer Deembedding Technique With Application to HBT Devices Characterization

Sami Bousnina, *Student Member, IEEE*, Chris Falt, Pierre Mandeville, *Member, IEEE*, Ammar B. Kouki, *Member, IEEE*, and Fadhel M. Ghannouchi, *Senior Member, IEEE*

***Abstract*—An accurate deembedding technique for on-wafer measurements of an active device's S-parameter is presented in this paper. This deembedding technique accounts in a systematic way for effect of all parasitic elements surrounding the device. These parasitic elements are modeled as a four-port network. Closed-form equations are derived for deembedding purposes of this four-port network. The proposed deembedding technique was used to extract small-signal model parameters of a 2×25 μm emitter GaInP/GaAs heterojunction bipolar transistor device, and excellent agreement between measured and model-simulated S-parameter was obtained up to 30 GHz.**

***Index Terms*—Device characterization, four-port network, microwave on-wafer measurements, S-parameter deembedding.**

I. Introduction

FOR THE development of microwave circuit applications using heterojunction bipolar transistor (HBT) devices, it is essential to use an accurate HBT's equivalent-circuit model to simulate circuit performances at microwave and millimeter-wave frequencies. The first stage of the modeling process is to deembed intrinsic device response from parasitic network associated with the on-wafer measurement environment. The normal approach is by means of a short, an open, a load, and a through test structures to characterize the device interconnects. This means that each device with a specific geometry and size will require an appropriate test structure to be fabricated [1], which is not usually possible in practice because of wafer area consumption. In addition, each device has to be measured with an appropriate calibration of the network analyzer. This further complicates the measurements for automated parameter extraction and affects speed of monitoring process. In practice, it is impossible to measure the S-parameter by putting the probes directly on the terminals of the intrinsic part of the device (see reference planes 3 and 4 in Fig. 1). This is due to smaller surface of these terminals compared to the probe size and to the fact that these terminals are not aligned with the probe tips. Furthermore, measuring the device with the probe tips so close can result in an extra coupling and leakage effects that influence accuracy of the measurements and extraction of the device's model parameters. It is well known that a more complete equivalent circuit for parasitics is necessary for accurate HBT device modeling at high frequencies. In addition, the parasitics of the equivalent-circuit model should also be easy to extract, which is not usually the case, and, in many cases, supplementary measurements have to be performed at specific bias conditions: reverse/forward-bias measurements [2], [3].

This paper presents an accurate deembedding technique suitable for quick evaluation of the device properties. In this technique, the parasitic elements surrounding the device are taken to be a generic four-port network without any need to model them with an equivalent circuit, as usually done in the previous techniques. These parasitic elements are then deembedded analytically using a derived closed-form equations.

This paper is organized as follows. In Section II, the procedure of deembedding the parasitic four-port network is presented. Section III then reports an experimental validation on HBT devices of the deembedding technique. Conclusions are given in Section IV.

II. Deembedding Method

The proposed deembedding method is outlined in the following three steps.

Step 1) Firstly, the measurement system has to be calibrated, defining reference planes for the S-parameter measurements at the end of the open pads (reference planes 1 and 2 in Fig. 1) using a standard calibration technique [i.e., short–open–load–through (SOLT)].

Step 2) Secondly, the measured data needs to be deembedded to bring the reference planes at the intrinsic device terminals (reference planes 3 and 4 in Fig. 1). The network to be deembedded from the measured data is provided in the form of a four-port S-parameter network modeled with an electromagnetic (EM) simulator where details about the device layout are supplied by the user. This four-port network in relation with the device model is represented in Fig. 2.

Step 3) Finally, the simulated four-port network is then deembedded analytically using a derived closed-form equations since the topology of the metalwork connected with the intrinsic device is

Manuscript received April 4, 2000.

S. Bousnina and F. M. Ghannouchi are with the Département de génie électrique et de génie informatique, École Polytechnique de Montréal, Montréal, QC, Canada H3V 1A2.

C. Falt and P. Mandeville are with Nortel Networks, Nepean, ON, Canada K1Y 4H7.

A. B. Kouki is with the École de technologie supériere, Montréal, QC, Canada H3C 1K3.

Publisher Item Identifier S 0018-9480(02)01151-1.

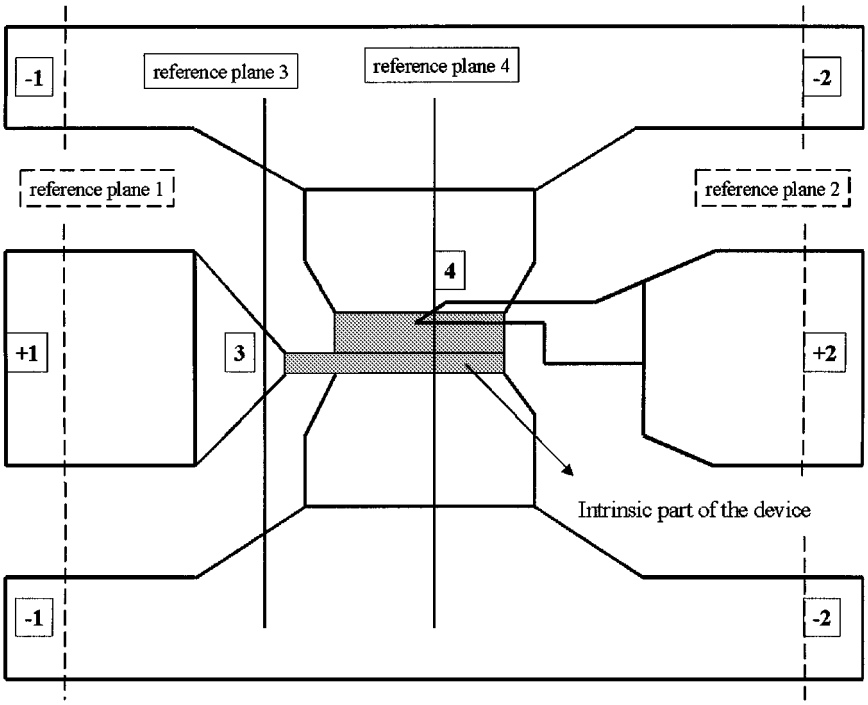

Fig. 1. Layout of a 2 × 25 μm^2 HBT device and the reference planes of EM simulation and SOLT calibration.

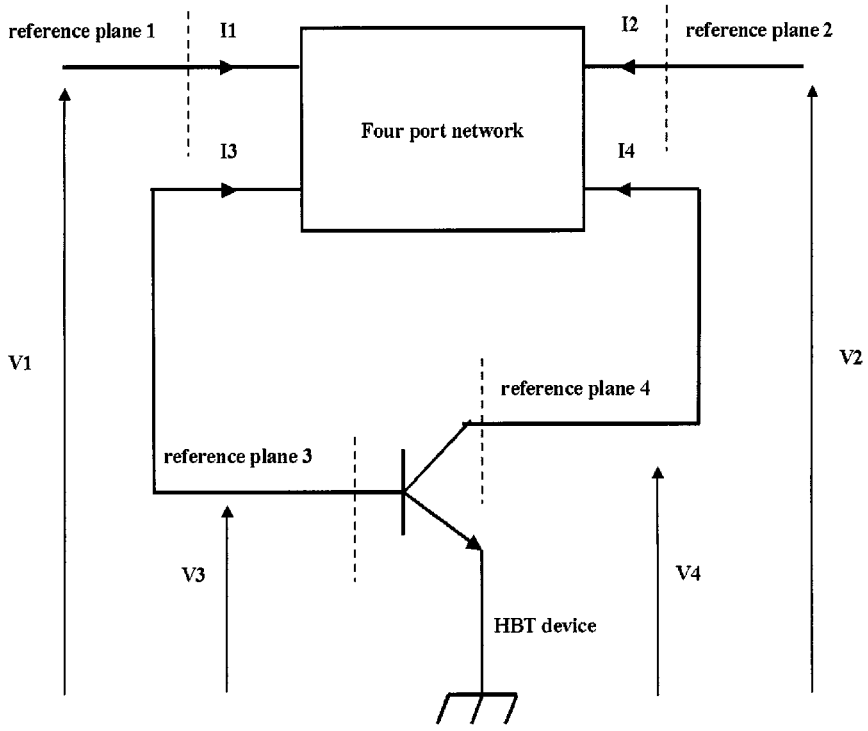

Fig. 2. Schematic of the four-port passive structure embedded with the HBT device.

not a standard topology (cascade, series, parallel). These equations are determined as follows.

The Z^G-parameters of the active device at reference planes 1 and 2 (see Fig. 1) are determined from the corresponding measured S-parameters. These Z^G parameters are defined as follows:

$$\begin{cases} V_1 = Z_{11}^G I_1 + Z_{12}^G I_2 \\ V_2 = Z_{21}^G I_1 + Z_{22}^G I_2. \end{cases} \tag{1}$$

The Z^D-parameters of the active device at reference planes 3 and 4 (see Fig. 1) are defined by the following equations:

$$\begin{cases} V_3 = Z_{11}^D(-I_3) + Z_{12}^D(-I_4) \\ V_4 = Z_{21}^D(-I_3) + Z_{22}^D(-I_4). \end{cases} \tag{2}$$

The Z^P-parameters of the four-port network are defined by the following equations:

$$\begin{cases} V_1 = Z_{11}^P I_1 + Z_{12}^P I_2 + Z_{13}^P I_3 + Z_{14}^P I_4 \\ V_2 = Z_{21}^P I_1 + Z_{22}^P I_2 + Z_{23}^P I_3 + Z_{24}^P I_4 \end{cases} \quad (3)$$

$$\begin{cases} V_3 = Z_{31}^P I_1 + Z_{32}^P I_2 + Z_{33}^P I_3 + Z_{34}^P I_4 \\ V_4 = Z_{41}^P I_1 + Z_{42}^P I_2 + Z_{43}^P I_3 + Z_{44}^P I_4. \end{cases} \quad (4)$$

From (1) and (3), we get

$$\begin{pmatrix} I_1 \\ I_2 \end{pmatrix} = \boldsymbol{A} \cdot \begin{pmatrix} I_3 \\ I_4 \end{pmatrix} \quad (5)$$

with

$$\boldsymbol{A} = \begin{bmatrix} Z_{11}^G - Z_{11}^P & Z_{12}^G - Z_{12}^P \\ Z_{21}^G - Z_{21}^P & Z_{22}^G - Z_{22}^P \end{bmatrix}^{-1} \cdot \begin{bmatrix} Z_{13}^P & Z_{14}^P \\ Z_{23}^P & Z_{24}^P \end{bmatrix}.$$

From (4) and (5), we get

$$\begin{pmatrix} V_3 \\ V_4 \end{pmatrix} = (\boldsymbol{B} \cdot \boldsymbol{A} + \boldsymbol{C}) \cdot \begin{pmatrix} I_3 \\ I_4 \end{pmatrix} \quad (6)$$

with

$$\boldsymbol{B} = \begin{bmatrix} Z_{31}^P & Z_{32}^P \\ Z_{41}^P & Z_{42}^P \end{bmatrix}$$

and

$$\boldsymbol{C} = \begin{bmatrix} Z_{33}^P & Z_{34}^P \\ Z_{43}^P & Z_{44}^P \end{bmatrix}.$$

By equalizing (6) to (2), one can determine the Z-parameter matrix of the active device at reference planes 3 and 4 (see Fig. 1) as follows:

$$\begin{bmatrix} Z_{11}^D & Z_{12}^D \\ Z_{21}^D & Z_{22}^D \end{bmatrix} = -(\boldsymbol{B} \cdot \boldsymbol{A} + \boldsymbol{C})$$

thus

$$Z_{11}^D = -Z_{31}^P \left(\frac{\left(-Z_{22}^G + Z_{22}^P\right) Z_{13}^P + \left(Z_{12}^G - Z_{12}^P\right) Z_{23}^P}{\text{Denom}} \right) - Z_{32}^P \left(\frac{\left(Z_{21}^G - Z_{21}^P\right) Z_{13}^P + \left(-Z_{11}^G + Z_{11}^P\right) Z_{23}^P}{\text{Denom}} \right) - Z_{33}^P$$

$$Z_{12}^D = -Z_{31}^P \left(\frac{\left(-Z_{22}^G + Z_{22}^P\right) Z_{14}^P + \left(Z_{12}^G - Z_{12}^P\right) Z_{24}^P}{\text{Denom}} \right) - Z_{32}^P \left(\frac{\left(Z_{21}^G - Z_{21}^P\right) Z_{14}^P + \left(-Z_{11}^G + Z_{11}^P\right) Z_{24}^P}{\text{Denom}} \right) - Z_{34}^P$$

$$Z_{21}^D = -Z_{41}^P \left(\frac{\left(-Z_{22}^G + Z_{22}^P\right) Z_{13}^P + \left(Z_{12}^G - Z_{12}^P\right) Z_{23}^P}{\text{Denom}} \right) - Z_{42}^P \left(\frac{\left(Z_{21}^G - Z_{21}^P\right) Z_{13}^P + \left(-Z_{11}^G + Z_{11}^P\right) Z_{23}^P}{\text{Denom}} \right) - Z_{43}^P$$

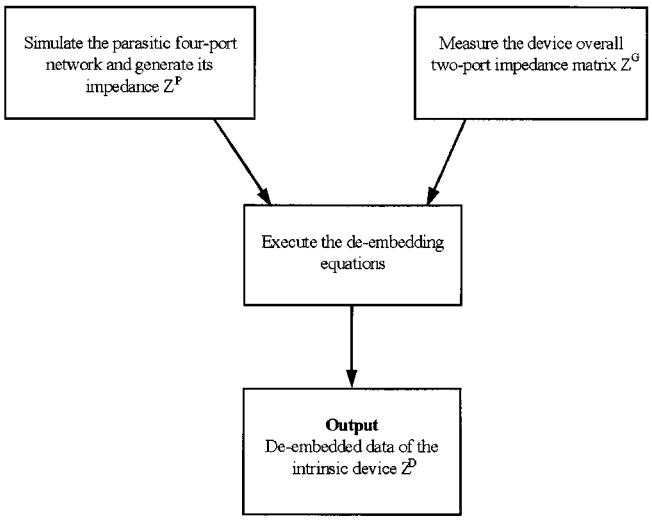

Fig. 3. Schematic diagram of the deembedding procedure.

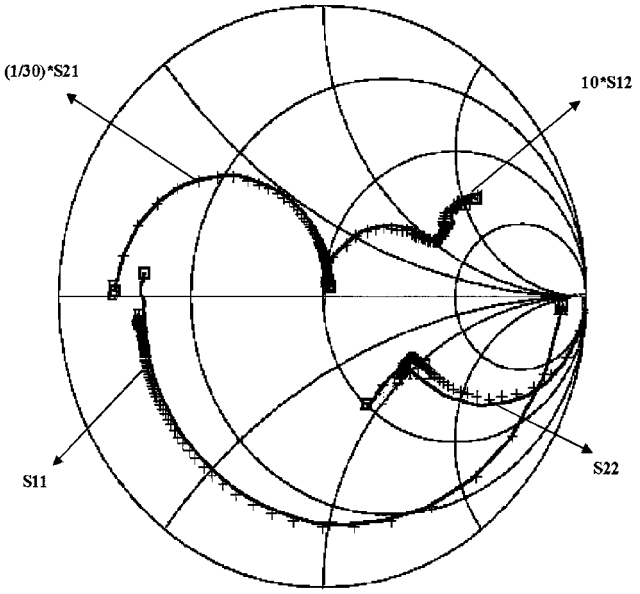

Fig. 4. Measured (−) and deembedded (+) S-parameter of a 2 × 25 μm^2 HBT from 40 MHz to 30 GHz.

$$Z_{22}^D = -Z_{41}^P \left(\frac{\left(-Z_{22}^G + Z_{22}^P\right) Z_{14}^P + \left(Z_{12}^G - Z_{12}^P\right) Z_{24}^P}{\text{Denom}} \right) - Z_{42}^P \left(\frac{\left(Z_{21}^G - Z_{21}^P\right) Z_{14}^P + \left(-Z_{11}^G + Z_{11}^P\right) Z_{24}^P}{\text{Denom}} \right) - Z_{44}^P$$

with

$$\text{Denom} = -Z_{11}^G Z_{22}^G + Z_{11}^G Z_{22}^P + Z_{11}^P Z_{22}^G - Z_{11}^P Z_{22}^P + Z_{12}^G Z_{21}^G - Z_{12}^G Z_{21}^P - Z_{12}^P Z_{21}^G + Z_{12}^P Z_{21}^P.$$

A schematic diagram resuming the deembedding procedure is presented in Fig. 3.

III. Experimental Validation

Several 2 × 25 μm^2 GaInP/GaAs HBT devices were measured, and deembedding results are presented. The measure-

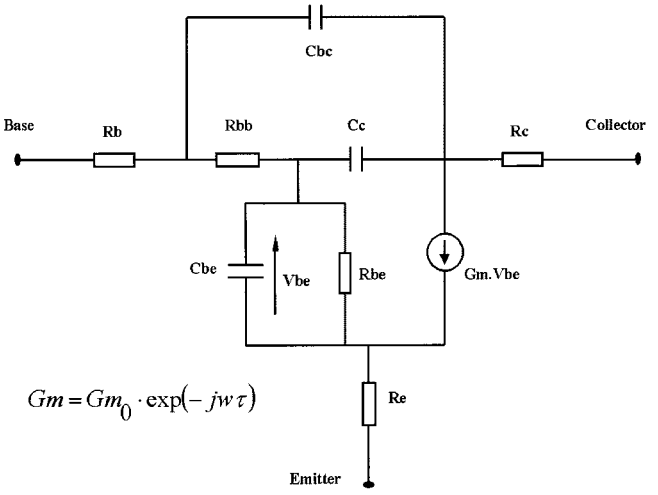

Fig. 5. Small-signal equivalent circuit of the GaInP/GaAs HBT.

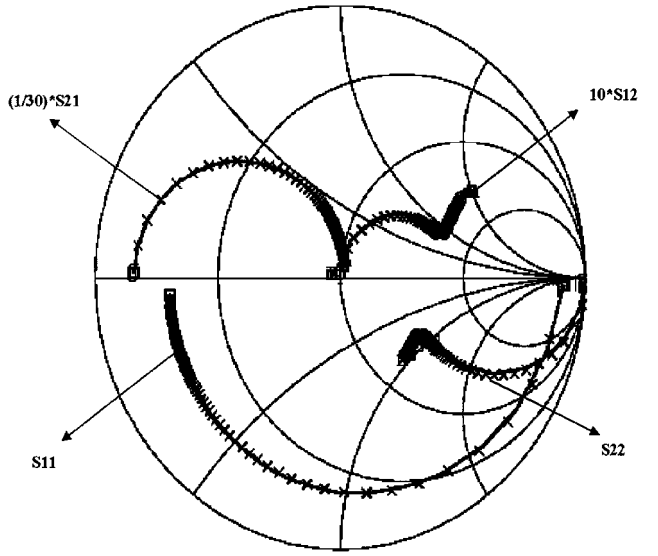

Fig. 6. Measured (−) and model-calculated (+) S-parameter of a $2 \times 25\,\mu\text{m}^2$ HBT from 40 MHz to 30 GHz.

ments were performed with a microwave probing system and a vector network analyzer (VNA) over the frequency range of 40 MHz to 30 GHz. Fig. 4 displays the measured S-parameters of the common-emitter HBT for the bias condition ($I_c = 10$ mA, $V_{ce} = 2$ V, $I_b = 50$ μA) and the corresponding deembedded S-parameters. The measurements show that the parasitics have both capacitive and inductive effects on S_{11} and S_{22}. S_{11} shows a capacitive behavior up to 30 GHz due to the relatively high value of base–emitter capacitance (C_{be}), and the inductive parasitic is responsible for the extra rotation in the raw data as the frequency increases. S_{22} also shows a smaller collector capacitance. S_{12} is smaller in magnitude and S_{21} has a smaller phase rotation. The significance of being able to deembed a four-port network is being able to account for the common terms between the base and collector interconnects, i.e., the emitter inductances or elements that contribute to S_{21} and S_{43}. The simulation of a 2×25 μm emitter HBT transistor interconnects had $|S_{21}|$ and $|S_{43}|$ equal to -26 dB at 30 GHz.

TABLE I
EXTRACTED PARAMETER VALUES OF THE SMALL-SIGNAL HBT MODEL
($I_c = 10$ mA, $V_{ce} = 2$ V, $I_b = 50$ μA)

Parameters	Extracted values
R_b (Ω)	1.5
R_c (Ω)	3.3
R_e (Ω)	1.1
R_{bb} (Ω)	7.5
C_c (fF)	22.7
C_{bc} (fF)	21.5
C_{be} (pF)	1.49
R_{be} (Ω)	565
τ (ps)	0.48
G_{m0} (Sie)	0.39

This deembedding method was also used in the extraction of the tested small-signal HBT devices where the intrinsic parameters of the model (Fig. 5) were determined by optimization using the HP Microwave Design System (HP MDS). Several trials were carried out in order to apply the same optimization routine to the measured data by using the same equivalent circuit and without deembedding the parasitic structure, but it was not possible to fit the measured S-parameters fully up to 30 GHz. This shows the necessity of taking into account the parasitic parameters when extracting the device small-signal model.

Fig. 6 presents the calculated and measured S-parameters after deembedding the passive structure surrounding the device. The extracted parameter values are listed in Table I. The excellent agreement of the fitted S-parameters from 40 MHz up to 30 GHz without taking into account any parasitic elements proves the validity and the accuracy of the new deembedding procedure. The residual error quantifying the accuracy of the data fitting was less then 1%. This residual error is defined according to the following function:

$$\|\vec{\varepsilon}\| = \frac{1}{4N} \sum_{i,j=1}^{2} \sum_{k=1}^{N} \frac{\left|S_{ij}^{m}(f_k) - S_{ij}^{c}(f_k)\right|}{\max_k \left(\left|S_{ij}^{m}(f_k)\right|\right)}$$

where N is the number of considered frequency points, $S_{ij}^{m}(f_k)$ is the measured S-parameter at the frequency f_k, and $S_{ij}^{c}(f_k)$ is the calculated corresponding S-parameter coefficient derived from extracted values of the model parameters.

IV. CONCLUSIONS

An accurate deembedding procedure for on-wafer high-frequency measurements has been developed and implemented. This procedure provides a systematic way to analytically deembed the parasitic elements surrounding the device including common elements between its input and output ports. This procedure uses a standard SOLT calibration technique to bring the measurement reference planes to the intrinsic device terminals, an EM simulation that allows the determination of the S-parameters of the parasitic four-port structure, and a closed-form equations to deembed the metalwork between the external and internal reference planes are used. The excellent agreement between deembedded-measured and model-fitted S-parameter up to 30 GHz of a 2×25 μm emitter GaInP/GaAs HBT device proves the validity and accuracy of the proposed technique.

ACKNOWLEDGMENT

The authors would like to thank the reviewers for their helpful comments and suggestions.

REFERENCES

[1] M. C. A. M. Koolen, J. A. M. Geelen, and M. P. J. G. Versleijen, "An improved de-embedding technique for on-wafer high-frequency characterization," in *IEEE Bipolar Circuits Technol. Meeting*, vol. 8.1, 1991, pp. 188–191.

[2] Y. Gobert, P. J. Tasker, and K. H. Bachem, "A physical, yet simple small-signal equivalent circuit for heterojunction bipolar transistor," *IEEE Trans. Microwave Theory Tech.*, vol. 45, pp. 149–153, Jan. 1997.

[3] S. Lee and A. Gopinath, "Parameter extraction technique for HBT equivalent circuit using cutoff mode measurement," *IEEE Trans. Microwave Theory Tech.*, vol. 40, pp. 574–577, Mar. 1992.

Sami Bousnina (S'01) was born in Elhamma, Tunisia. He received the Electrical Engineering degree and D.E.A. degree from the Ecole Nationale des Ingénieurs de Tunis, Tunis, Tunisia, and is currently working toward the Ph.D. degree at the Ecole Polytechnique de Montréal, Montréal, QC, Canada.

His main interests include characterization and modeling of microwave semiconductor active devices (HBTs and FETs) and design of high-efficiency power amplifiers. From May to November 1999, he was with Nortel Networks, Ottawa, ON, Canada, where he was an Intern involved with the HBT devices characterization and small-signal modeling.

Mr. Bousnina was a student finalist in the Student Paper Competition of the 2000 IEEE Microwave Theory and Techniques Society (IEEE MTT-S). He was the recipient of the National Scholarship presented by the Tunisian Government (1998–2001).

Chris Falt received the B.Sc. degree in engineering physics from the Queen's University, Kingston, ON, Canada, in 1987.

In 1987, he joined Nortel Networks, Ottawa, ON, Canada, where he designs GaAs integrated-circuit (IC) packages and has recently designed GaAs HBT monolithic microwave integrated circuits (MMICs) for high-speed optical systems.

Pierre Mandeville (S'90–M'92) received the Ph.D. degree in electrical engineering from Cornell University, Ithaca, NY, in in 1993.

In 1985, he joined Nortel Networks (then Bell Northern Research), Nepean, ON, Canada, where he was involved in molecular beam epitaxy and later chemical beam epitaxy of optoelectronic and high-speed electronic structures. In 1996, he joined the high-speed circuit design team and currently manages the Fiber Circuit Development Group.

Ammar B. Kouki (S'89–M'90), photograph and biography not available at time of publication.

Fadhel M. Ghannouchi (S'84–M'88–SM'93) received the B.Eng. degree in engineering physics and the M.S. and Ph.D. degrees in electrical engineering from the Ecole Polytechnique de Montreál, Montreál, QC, Canada, in 1983, 1984, and 1987, respectively.

He is currently a Professor with the Département de génie électrique et de génie informatique, Ecole Polytechnique de Montreál, where, since 1984, he has taught electromagnetics and microwave theory and techniques. He has provided consulting services to a number of microwave companies. He is also the founder of AmpliX Inc., Montréal, QC, Canada, a company that offer linearization products and services to wireless and satcom equipment manufacturers. His research interests are in the areas of microwave/millimeter-wave instrumentation and measurements, nonlinear modeling of microwave active devices, and design of power and spectrum-efficient microwave amplification systems.

Dr. Ghannouchi is a Registered Professional Engineer in the province of Quebec, Canada. He is on the editorial board of the IEEE TRANSACTIONS ON MICROWAVE THEORY AND TECHNIQUES and has served on the Technical Committees of several international conferences and symposiums.